Experimental research on direct expansion heat pump flue gas waste heat recovery and humidification nitrogen reduction system

9011 words in total

Experimental Research on Direct Expansion Heat Pump Flue Gas Waste Heat Recovery and Humidification Nitrogen Reduction System

Qunli Zhang [a,b,*], Haotian Huang [a,b], Hongbao Zhai [b, c], Wenqiang Zhao [a,b], Xiaoshu Lü [b,d,e]

[a] *Beijing Municipality Key Lab of Heating, Gas Supply, Ventilation and Air Conditioning Engineering, Beijing University of Civil Engineering and Architecture, Beijing 100044, China*

[b] *Collaborative Innovation Center of Energy Conservation & Emission Reduction and Sustainable Urban-Rural Development in Beijing, Beijing 100044, China*

[c] *Beijing Gas Group Co. Ltd*

[d] *Department of Electrical Engineering and Energy Technology, University of Vaasa, P.O.Box 700, FIN-65101, Vaasa, Finland*

[e] *Department of Civil Engineering, Aalto University, P.O.Box 12100, FIN-02130, Espoo, Finland*

Highlights

- A humidification combustion system coupled with waste heat recovery technology is proposed
- Effects of Air humidity on heating efficiency and clean emissions are revealed
- The improvement of the heating capacity of the system by the heat pump is studied
- Flue gas temperature can be reduced to 24.46℃ while NOx emissions are 39.66 mg/m^3

Abstract

In order to solve the heat loss and the pollution of gas boilers, a synergistic system consisting of waste heat recovery tower and air humidification tower is proposed. Increasing in moisture content of the air can inhibit the generation of nitrogen oxides and increase the dew point of the flue gas, which is beneficial to the utilization of the waste heat from the flue gas. More heat is absorbed by the humidification water at the fin heat exchanger after the flue gas enters the waste heat recovery tower, which enhances the heat and mass exchange process in the air humidification tower. But the performance of the heat pump was found to show a downward trend, indicating a competitive relationship between nitrogen oxides reduction and waste heat recovery. Under the optimal condition, the experimental system can reduce nitrogen oxides emissions by 62.35%, and the exhaust gas temperature can be reduced to 24.46 ℃. The heat pump can recover 6.94% heat while maintaining a minimum nitrogen oxides emission of 39.66 mg/m^3. The heat pump makes more heat from the fuel to enter the heating network, which improves the heating efficiency of the boiler system. The system can meet the high-efficiency and clean production requirements of the energy system at the same time.

Keywords: Gas boiler; Combustion-air humidification; Waste heat recovery; NOx emission reduction; Synergy.

	Abbreviations	*PP*	Payback period
AHP	Absorption heat pump	*Q*	Heat
CA	Combustion-air	*R*	Liquid-Gas ratio
CAH	Combustion-air humidification	*V*	Standard molar volume of gas
DHE	Direct heat exchanger	η	Efficiency
FGR	Flue gas recirculation		**Subscripts**
FTHE	Finned tube heat exchanger	*ca*	Combustion-air
HP	Heat pump	*cw*	Condensed water
IDHE	Indirect heat exchanger	*d*	Dry components in gas
OFC	Oxy-fuel combustion	*e*	Electricity
PC	Premixed combustion	*eg*	Exhaust gas
SC	Staged combustion	*fg*	Flue gas
WH	Waste heat	*g*	Mass flow of the input gas
WHR	Waste heat recovery	*h*	Mass transfer of CAH water to CA
NOx	Nitrogen oxides	*hca*	Humidified combustion-air
	Nomenclature	*hw*	Humidified water
B	Flow of natural gas	*hn*	Heat network
C	Component concentration	*m*	Mass concentration
cp	Constant pressure specific heat	*net,ar*	Low calorific value
d	Moisture content	*PPM*	PPM concentration
E	Power consumption	*r*	Reaction to product
h	Enthalpy	*rh*	Recovered heat
I	Initial investment	*rw*	WHR water
m	Mass Flow	*s*	Amount of savings
M	Molecular mass	*u*	Heat users
P	Unit price of energy	*v*	Vapor

1. Introduction

The Paris Agreement urges changes in energy systems for cleaner production, higher efficiency and lower carbon emission(Cai et al., 2018). However, the consumption ratio of high-carbon fuels in energy structure is still in an absolute dominant position in China(Chen et al., 2019). In 2021, China's annual gas consumption increased by 12.5%, which was the highest in history. Natural gas applications are mainly concentrated in northern China. In Beijing, the gas consumption in 2021 has already reached 18.8 billion m^3, and more than half of gas was used for heating.

The exhaust gas temperature of gas boilers often exceeds 150 ℃(Zhao et al., 2016), indicating a large amount of heat wasted (Yang et al., 2018). Most of the waste heat (WH) is carried by vapor(Qu et al., 2014) as latent heat(Chen, H. et al., 2017). According to statistics, burning 1Nm^3 of gas causes about 3.6 MJ of latent heat to be wasted(Wang et al., 2013). Recovering and utilizing the WH are beneficial to improve the heating capacity of the boiler system(Wei et al., 2017), reduce energy consumption(Terhan and Comakli, 2016) and CO_2 emissions(Su et al., 2021). The wide application of gas boilers also leads to an increase in nitrogen oxides (NOx) emissions(Yi et al., 2019), which may lead to serious environmental problems such as acid rain and photochemical smog(El Sheikh et al., 2019). In addition, the impact of pollutants from boilers on human health cannot be ignored(Cansino et al., 2019), especially on newborns(IHME, 2019). A survey of pollutant hazards in Spain

suggested that reducing local pollutant levels to WHO standards could prevent 182 deaths and reduce economic loss (Roman-Collado and de Reyna, 2019). Therefore, reducing the NOx emissions and improving the heating efficiency is an important direction for the optimization of gas boiler systems.

Direct(Shang et al., 2017) and indirect(Zhu et al., 2014) heat exchangers (DHE, IDHE) are used in waste heat recovery (WHR) to increase boiler efficiency commonly. The efficiency of the WHR generally depends on the contact area, the heat transfer boundary conditions, and the material of the heat exchanger(Chen, W. et al., 2017). IDHE with multi-stage recovery theory can increase boiler efficiency to 103.4%(Chen, W. et al., 2017). Rational structural designs also make WHR efficiency higher (Khaled and Ramadan, 2017). The flue gas is acidic, and materials with corrosion resistance and lower thermal resistance are needed(Lion et al., 2020). The recovery of latent heat requires a cold source with the temperature below the dew point of flue gas(Kuck, 1996), which is hard to find in most boiler houses.

It has been proven that applying a heat pump (HP) can avoid the limitation imposed by the temperature of the cold source(Men et al., 2021). WHR systems with compression HPs can improve heating efficiency by 3%-21%(Hebenstreit et al., 2014), and the exhaust gas temperature can be reduced to 30°C(van de Bor et al., 2015). A large compression HP was used to recover the WH in the steel plant, and the COP exceeds 6(Hu et al., 2022). Absorption heat pumps (AHP) are driven by heat and applied without consideration of the electrical system(Lu et al., 2019). Study has found that a system consisting of AHP with DHE can increase the total heat capacity by 12%(Zhu et al., 2014). However, systems of AHPs are complicated and cannot maintain a high efficiency when the evaporation temperature is low. In contrast, the compression HP is simpler, which is suitable for application in small heating boiler systems.

The common low-NOx combustion technologies include premixed combustion (PC), flue gas recirculation (FGR), staged combustion (SC) and oxy-fuel combustion (OFC). In addition, there are denitration technologies applied to large boiler system because of the requirments of large site for laying dedicated equipment and high costs (Cheng and Zhang, 2018). Studies have shown that changing the combustion-air (CA) port of the SC system and the mixing method of combustion components can reduce NOx emissions(Wang et al., 2019). By changing the position of the CA injectors, NOx emissions can be reduced by 23%(Shi et al., 2018). NOx formation is significantly suppressed in reducing atmospheres (Carroll et al., 2015). Constructing an insufficient combustion zone(Wu et al., 2020) and adding flue gas(Sidorkin et al., 2019), CO_2(Feser and Gupta, 2018), H_2O(Zhou et al., 2021) into the furnace can inhibit the formation of NOx. But CO_2 has high specific heat capacity and low thermal diffusivity, and excessive CO_2 dilution affects flame stability, which is also reflected in FGR. In contrast, H_2O is a better choice(Vandel et al., 2020). There are many ways to add H_2O into furnace, including direct injection and spray to CA(Shahpouri and Houshfar, 2019). However, more heat is wasted with the flue gas(Lee and Kim, 2020) while achieving a higher NOx removal rate by humidification combustion (HC), which results in a lower boiler efficiency. Many low-NOx combustion technologies have strict requirement for the coordination of combustion stability and NOx removal rate. But these technologies rarely take thermal efficiency into account(Gamrat et al., 2016), some even cause additional negative effects(Zhang et al., 2020).

In order to achieve synergy between clean emissions and efficient heating, we innovatively proposed a new form of WH utilization, which is to heat CAH water to ensure that CA carries more moisture, thereby reducing NOx emissions. The increase of the moisture content of the flue gas increases its dew point. Under the combined effect of high dew point temperature and HP, the requirement of WHR on a low-temperature cold source in gas boilers are no longer as strict as it in traditional condensation boilers. Furthermore, the synergistic mechanism of NOx emissions, system efficiency and boiler efficiency was revealed. The system can achieve the tasks of NOx reduction and efficiency improvement, which is a feasible way to complete clean and efficient production.

2. Experiment System and methods

2.1 System Profile

The system consists of a gas boiler, a CAH tower, a compression HP a WHR tower and a finned tube heat exchanger (FTHE). The FTHE and the direct expansion evaporator of the HP are arranged in the WHR tower, as shown in **Figure 1**.It's located in an laboratory in Beijing. The heating performance and pollutant emission were experimentally studied. The flow chart of the system is shown in **Figure 2**.

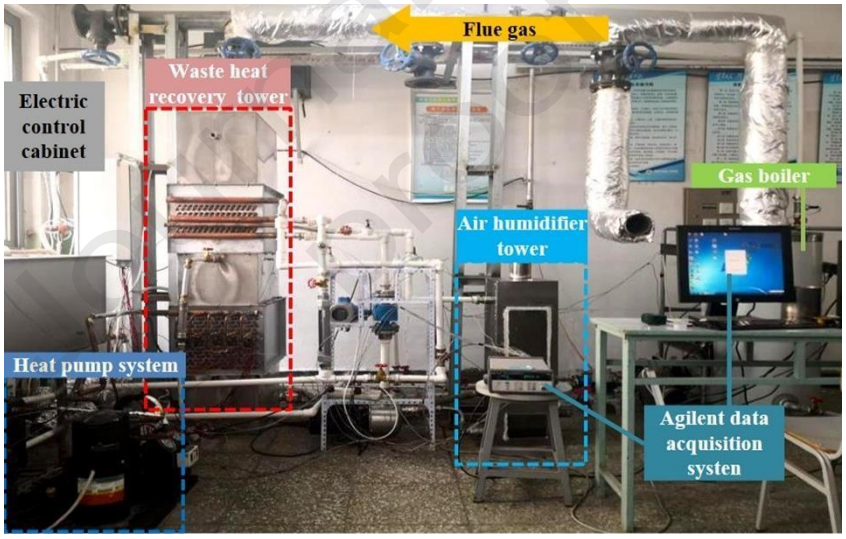

Fig.1 Appearance of synergistic system

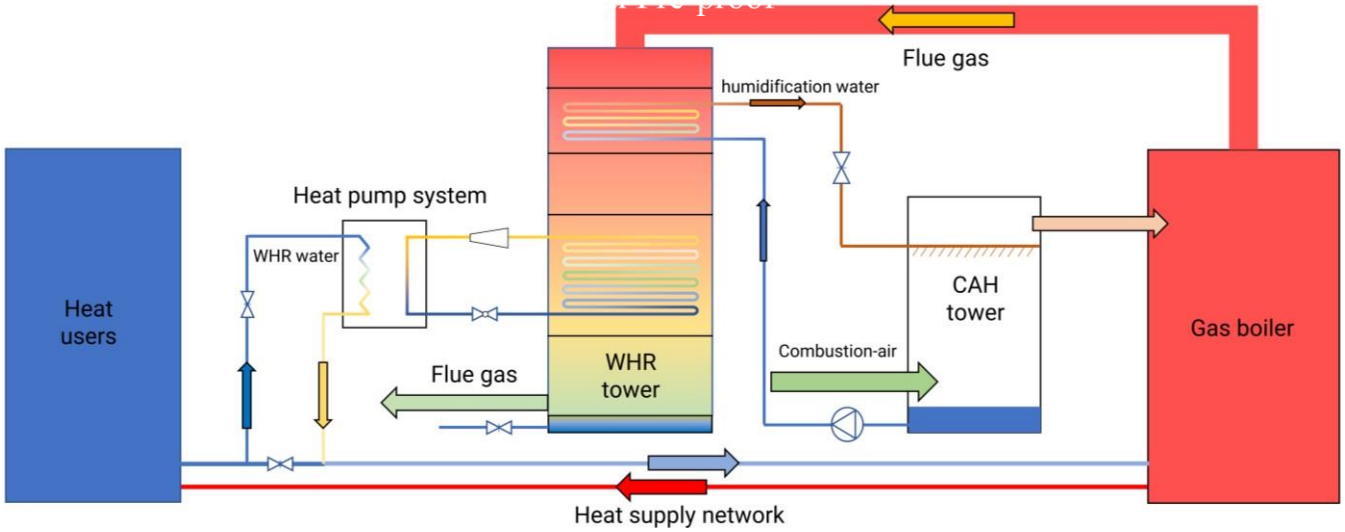

Fig.2 Flow chart of synergistic system

The heat input to the boiler is transferred to to the heating network and flue gas.

The flue gas would be sent to the WHR tower later and releases heat at the FTHE and the evaporator of the HP. There is a large amount of vapor condensed in the heat exchange process. The condensed water is collected at the bottom of the tower. Dry and low-temperature flue gas is discharged at the bottom of the WHR tower.

In the WHR tower, the flue gas first passes through the FTHE. The CAH water is heated at the FTHE, and then flows into the CAH tower for heat and mass transfer with CA. The high-temperature and high-humidity CA is sent into the boiler to participate in combustion process. Other CAH water that isn't sent into boiler is collected at the bottom of the CAH tower. It would be sent into the FTHE to absorb heat again.

At the evaporator of the HP, the WH is further absorbed. These absorbed WH will be transferred to the WHR water at the HP condenser. The WHR water is part of the back water of the heat network. The heat transferred by the HP is also transferred to the heat network by the WHR water.

2.2 Experimental Conditions

The parameters of the gas boiler are shown in **Table 1**.

Table 1 Parameters of the gas boiler

Name	Value
Boiler capacity	58kW
Rated inlet/ outlet water temperature	65°C /85°C
Gas consumption (100% load)	5.7Nm^3/h
Excess air ratio	1.2
Flue gas temperature	200°C-210°C

The boiler's original operating conditions and parameters were tested when the back water of the heating network is 40 °C. In this part, the CAH water flow is 0 L/h and the HP is turned off. The results are shown in **Table 2**.

Table 2 Boiler's original working efficiency and NOx emission

Boiler load (%)	Heat network water flow (L/h)	Heat network temperature difference (K)	Boiler heat supply (kW)	NOx emissions (mg/m^3)
90	1863.77	24.54	46.36	100.66
75	1867.46	21.69	38.76	90.34

The test points required for the experiment are shown in **Figure 3**. In the CAH tower, the effects of CAH water flow and temperature on CA humidity, temperature and NOx content in flue gas were investigated. The WHR tower was mainly used to find out the factors affecting the performance of WHR and the synergistic mechanism of NOx reduction. Since the heat obtained by CAH water at the FTHE is used in the CAH tower instead of the heat network, this part of the heat is not counted in the recovered WH. the WH actually utilized is the heat absorbed by the HP. Therefore, the study of the WHR subsystem was divided into three parts:

1) effect of the temperature and flow of WHR water on the heat obtained;

2) effect of CAH water flow on the heat obtained by the WHR water;

3) effect of the moisture content of the CA on the heat transfer process in the WHR tower.

The main test equipments and parameters of the system are shown in **Table 3**.

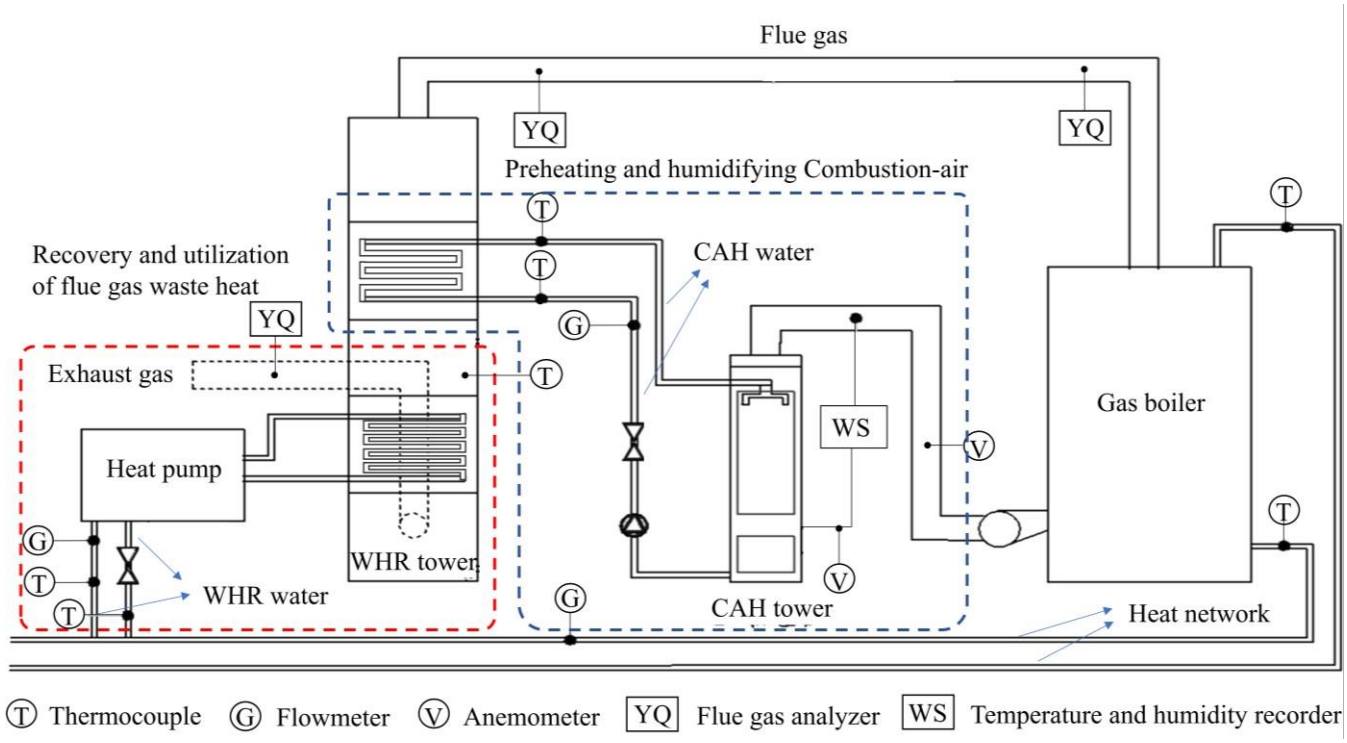

Fig.3 WHR and NOx emission reduction performance test points

Table 3 Experimental test parameters and instruments

Parameter	Equipment	Model	Unit	Accuracy
Flue gas temperature	Flue gas analyzer	Testo 340	°C	±1°C
NO concentration			ppm	±5PPM
Water temperature	Thermocouple	T-type thermocouple	°C	±0.75% F.S(-200~350°C)
Water flow	Electromagnetic Flowmeter	LDYD3-032-16-1-1	L/h	±0.5% F.S(0~2,000L/h)
Air temperature	Temperature and humidity recorder	WWSZY-1	°C	±0.3°C
Air humidity ratio			%	±2%RH(0~100% RH)
Air velocity	Digital Anemometer	AS8336	m/s	±0.03m/s

2.3 System Analysis Model

2.3.1 Composition Equations of the System

The mass flow of each component is calculated under standard conditions. The mass flow of each gas is taken as the sum of H_2O and dry components in the gas.

$$m_i = m_{i,v} + m_{i,d} \tag{1}$$

$$d_i = \frac{1000 \cdot m_{i,v}}{m_{i,d}} \tag{2}$$

Where, i is the gas to be tested, including flue gas, exhaust gas, CA and humidified CA; m_i is the mass flow of i, kg/s; $m_{i,v}$ is the vapor content in i, kg/s; $m_{i,d}$ is the content of dry components in i, kg/s; d_i is the moisture content of i, $g/kg_{dry,air}$.

For the calculation of the moisture content of the CA, we refer to the results of a large-scale physical property calculation query platform(November 14, 2022). This platform summarizes the physical property equations of many substance, REFPROP and SUPERTRAPP model, and provides calculation and query services of physical properties for many Chinese universities.

Mass transfer in the CAH tower is calculated as the difference between the moisture content of the CA and humidified CA.

$$m_h = \frac{d_{hca} \cdot m_{hca,d} - d_{ca} \cdot m_{ca,d}}{1000} \tag{3}$$

Where, m_h is the mass transfer of CAH water to CA, kg/s; d_{hca} and d_{ca} are moisture content of CA and humidified CA, $g/kg_{dry,air}$; $m_{ca,d}$ and $m_{hca,d}$ is the content of dry components in CA and humidified CA, kg/s.

The calculation of mass flow follows the principle of mass conservation. The vapor carried by the flue gas comes from the humidified CA and the combustion reaction. The fuel for the combustion reaction is seen as pure methane gas. The mass of condensed water in the WHR tower is the difference between the mass of vapor carried by the high-temperature flue gas and the exhaust gas.

$$m_{fg} = m_{eg} + m_{cw} = m_{hca} + m_g \tag{4}$$

$$m_{r,v} = \frac{\alpha \cdot M_{H_2O} \cdot m_g}{M_g} \tag{5}$$

$$m_{fg,v} = m_{r,v} + m_{hca,v} \tag{6}$$

$$m_{fg,v} = m_{eg,v} + m_{cw} \tag{7}$$

Where, m_{fg} is the mass flow of flue gas, kg/s; m_{eg} is the mass flow of exhaust gas, kg/s; m_{cw} is the mass flow of condensed water in the WHR tower, kg/s; m_{hca} is the mass flow of humidified CA, kg/s; m_g is the mass flow of the methane,

kg/s; $m_{r,v}$ is the water generated for combustion reaction, kg/s; α is the molar ratio of H_2O to methane in the reaction, 2; M_{H2O} is the molecular mass of H_2O, 18g/mol; M_g is the molecular mass of methane, 16 g/mol; m_g is the input methane mass, kg/s; $m_{fg,v}$ and $m_{hca,v}$ are the H_2O in the flue gas and humidified CA, kg/s; $m_{eg,v}$ is vapor content of the exhaust gas, kg/s.

2.3.2 Energy Equations of the System

In the boiler, the heat from the gas and CA is transfered to the flue gas and heat network. The WH flows to CAH water, HP, condensed water, exhaust gas. There is a certain heat loss in the WHR tower.

$$Q_{hca} + Q_g = Q_{hn} + Q_{hw} + Q_{rh} + Q_{cw} + Q_{eg} + Q_{loss} \tag{8}$$

$$Q_g = \frac{B \times Q_{net,ar}}{3600} \tag{9}$$

$$Q_{hca} = m_{hca,d} \times h_{hca} \tag{10}$$

Where, Q_{hca} is the heat input by humidified CA, kW; Q_g is the heat input by natural gas, kW; Q_{hw} is the heat gain of CAH water, kW; Q_{hn} is the heat gain of the heat network from boiler, kW; Q_{rh} is the heat recovered by HP, kW; Q_{cw} is the heat carried away by condensed water, kW; Q_{eg} is the heat of exhaust gas, kW; Q_{loss} is the heat loss of the system, kW; B is the input of gas, related to the load of the boiler, Nm^3/h; $Q_{net,ar}$ is low calorific value of gas, kJ/m^3; h_{hca} is enthalpy of humidified CA, $kJ/kg_{dry\ air}$. The enthalpy can be calculated by $1.006 \cdot t + (2501 + 1.86 \cdot t) \cdot d$(ASHRAE, 2013), where, t and d are the temperature and moisture content of the calculation object. The heat transfer in the humidification process of CA is also calculated by enthalpy:

$$Q_h = m_{hca,d} \times h_{hca} - m_{ca,d} \times h_{ca} \tag{11}$$

Where, h_{ca} is enthalpy of CA, $kJ/kg_{dry\ air}$.

There are two main heat exchange processes in the WHR tower: Q_{hw} and Q_{rh}. In the process of calculating the recovered heat, HP is regarded as an ideal heat transfer system. This part of the heat is calculated by the COP of HP (Hebenstreit et al., 2014).

$$Q_{hw} = c_p \times m_{hw} \times (t_{hw,\,out} - t_{hw,\,in}) \tag{12}$$

$$Q_{rw} = c_p \times m_{rw} \times (t_{rw,\,out} - t_{rw,\,in}) \tag{13}$$

$$Q_{rw} = Q_{rh} + E_{hp} \tag{14}$$

$$\mathrm{COP} = \frac{Q_{rw}}{E_{hp}} \tag{15}$$

Where, c_p is constant pressure specific heat of water, kJ/(kg•°C); m_{hw} is the mass flow rate of CAH water, kg/s; $t_{hw,\,out}$ and $t_{hw,\,in}$ are temperature of CAH water sent into and out of the WHR tower, °C; m_{rw} is the mass flow rate of WHR water, kg/s; $t_{rw,\,out}$ and $t_{rw,\,in}$ are temperatures of the WHR water sent into and out of the HP, °C; E_{hp} is the power consumption of the HP, kW.

The WHR efficiency and boiler heating efficiency are as follows:

$$h_{rh} = \frac{Q_{rh}}{Q_g} \times 100\% \tag{16}$$

$$h_{hn} = \frac{Q_{hn}}{Q_g} \times 100\% \tag{17}$$

$$Q_{hn} = c_p \times m_{hn} \times (t_{bo,\,out} - t_{bo,\,in}) \tag{18}$$

Where, h_{rh} is the WHR efficiency, %; h_{hn} is the boiler heating efficiency, %; m_{hn} is mass flow of heat network water, kj/m^3; $t_{bo,out}$ and $t_{bo,in}$ are temperatures of heat network water sent into and out of the boiler, °C.

2.3.2 Analysis and Evaluation Models

The research on system operation adjustment based on heat users' load has not been carried out. It's hard to analyze the system economy based on an actual heat demand environment. So we defined a building model, which has the following characteristics:

1) The building area is 300m^2, the heat demand per unit area is 60w/m^2, and the building has a constant daily heat demand;

2) The end of the heat network is an energy storage device (ESD), and the water from the heat network does not directly participate in the heat exchange process in the building;

3) There is no heat loss in the heat transfer process of the heat network and ESD;

4) The temperature change of the heat network water after the boiler is stopped is not considered;

5) The system operates every year for 121 days.

Since the heat source of the building is ESD, the boiler system would stop working after it produced enough heat to meet the total demand of the building in one day. The payback period calculation for the system takes into account the benefits of increased efficiency and the cost of additional power consumption. Since this system is still in the stage of laboratory research, the labor cost during system operation has not been considered yet. The conclusions in this section are for reference only.

$$T = \frac{Q_B}{Q_{rw} + Q_{hn}} \tag{19}$$

$$\Delta T = \frac{Q_B}{Q_{hn}} - T \tag{20}$$

Where, T is the system daily running time, h; Q_B is the daily heat demand of the building, 432kW*h; ΔT is the reduction of daily running time caused by the improvement of thermal efficiency, h. The system operates under 90% load, and the reduction in running time leads to a reduction in gas consumption:

$$\Delta B = \Delta T \times B \tag{21}$$

$$S = \Delta B \times P_{gas} \tag{22}$$

Where, ΔB is daily reduced gas consumption, Nm^3; S is daily gas-savings, CNY; P_{gas} is the unit price for gas, CNY/Nm^3.

There are several power consumers in the system, including CAH water pump and HP. The heat exchanger in the WHR tower increases the resistance of flue gas flow, and the fan is installed at the outlet of the WHR tower. In addition, the heat network water is divided before the HP. The flow to the HP rejoins after the heat exchange process. This is additional pump energy

consumption.

$$COST_i = E_i \times T \times P_i \quad (23)$$

$$PP = \frac{I}{S - \sum COST_i} \quad (24)$$

Where, $COST_i$ is the daily incremental cost in operation because of i, CNY; E_i is the power or increased power of these devices, kW, which was measured experimentally; P_i is the unit price for i, CNY/kW*h; PP is the payback period of the system, a; I is the system initial investment, CNY.

2.4 Measurement Uncertainty Analysis

This chapter is used for the screening of experimental data and proof of accuracy. Uncertainty and uncertainty propagation(Glen, April 14, 2021) are used to verify the accuracy of experimental conclusions. The recording interval of experimental data is 2 seconds.

Eq 13 is used for the uncertainty analysis of WHR. The uncertainty of the electromagnetic flowmeter measurement is 0.5%, and the thermocouple measurement is 0.75%. Under the condition of 90% load, the temperatures of WHR water flowing through the HP condenser are 39.43 °C and 43.04 °C, with uncertainties of 0.08 °C and 0.09 °C. The temperature difference before and after the WHR passed through the HP condenser is 3.61°C, the uncertainty propagation is 0.12°C, and the relative propagation is 3.32%. Since c_p is a constant, the measurement error of the electromagnetic flowmeter is 0.5%, and the uncertainty of the heat gain of the WHR water is 3.24%.

Eq 12 was used for uncertainty analysis of the heat gain of CAH water. Under the conditions of 90% load, the temperatures of the CAH water entered and left the FTHE are 45.09 °C and 47.38 °C, and the uncertainties are both 0.04 °C. The temperature difference is 2.29°C and the uncertainty propagation is 2.49%. The uncertainty spread for heat gain of CAH wateris 2.49%.

NOx emissions were recorded every 5 seconds by flue gas analyzer. The NO_2 content in the flue gas is little and it's soluble in water easily(Li et al., 2019). The measured value of NO was used as an indicator of boiler NOx emissions in this experiment as the vapor content of flue gas under the humidification condition was significantly higher than it under the original boiler condition. Considering that NO would be oxidized to NO_2 by O_2 finally, the NOx emission mass concentration is calculated by the molecular mass of NO_2:

$$C_{m,\,NO_x} = \frac{M_{NO_2} \cdot C_{PPM,\,NO}}{V} \quad (25)$$

Where, $C_{m,\,NO_x}$ is the mass concentration of NOx，mg/m^3; $C_{PPM,NO}$、C_{PPM,NO_2} is the volume fraction of NO and NO_2, PPM; M_{NO_2} is the molar mass of NO_2, 46g/mol; V is standard molar volume of gas, 22.4L/mol. Under 90% working

condition, the lowest measured NOx emission is 39.66mg/m^3. At this time, the measurement uncertainty of NO is 0.13PPM, which is 0.65%.

The uncertainty calculation of the whole experimental process data reflected in the analysis is similar to the above.

3. Results and discussion

3.1 Humidification Process in CAH tower

3.1.1 Mass Transfer in the Humidification Process

The influence of spraying process on CA humidity is mainly reflected in relative humidity (RH) and temperature. Temperature is an indicator of the ability of CA to carry water. RH reflects how close the CA moisture content is to this capacity. In the experiment, the temperature and the RH of the CA at the inlet and outlet of the CAH tower were measured, as shown in **Table 4** and **Table 5**. It is found that the CAH tower can always make CA close to saturation.

Table 4. Effects of spray humidification on CA moisture content and temperature (90% load)

CAH water			CA before humidification		CA after humidification		
Flow	Temperature (℃)		Temperature	RH	Temperature	RH	Moisture content
(L/h)	Into tower	Out of tower	(℃)	(%)			(℃)
0			19.19	22.54			
232	56.30	47.24	20.47	21.01			33.62
379	52.88	45.99	21.58	22.80			38.34
640	50.99	46.22	22.16	23.96			40.48
935	49.26	45.86	21.36	23.77			42.46
1,257	48.20	45.51	21.15	24.87			43.38
1,543	47.48	45.09	21.40	23.11			44.15

Table 5. Effects of spray humidification on CA moisture content and temperature (75% load)

CAH water			CA before humidification		CA after humidification		
Flow	Temperature (℃)		Temperature	RH	Temperature	RH	Moisture content
(L/h)	Into tower	Out of tower	(℃)	(%)	(℃)	(%)	($g/kg_{dry,air}$)
0			17.54	32.62			4.04
255	46.73	40.99	18.27	40.37	31.21	96.87	28.28
382	43.38	39.15	15.10	43.30	32.21	97.06	30.08
622	42.04	39.13	20.27	28.20	34.28	97.04	33.97
950	40.15	38.27	19.72	32.83	35.41	96.71	36.16
1,245	39.13	37.65	18.84	36.33	35.69	96.95	36.85
1,523	39.28	37.97	20.19	30.57	36.73	96.90	39.13

The CA under a higher load can often be heated to higher temperatures. The heat and mass exchange intensity during the spraying process is obviously related to the spraying water flow. The CA under a higher CAH water flow obtained higher temperature and moisture content. It may be related to the contact time between the CAH water and the CA.

The change of load causes the change of CA flow. Using the CAH water flow to describe and analyze the experimental conclusions can not clearly explain the impact of humidification on the system when the load changes. Therefore, the ratio of the CA flow to the CAH water flow is defined for the analysis of the experimental data:

$$R_{liquid-gas} = \frac{m_{hw}}{m_{CA}} \tag{26}$$

The CA under a high load often carries more water and can be heated to higher temperature, as shown in **Figure 4**, which shows that lower CAH water flow under lower load, not the CAH water temperature, is the limiting factor for humidification performance. The decrease of load also causes the temperature of flue gas decreased. Then, the heat gain of CAH water decreases, which is not conducive to the humidification of CA. The temperature difference between the humidified CA and the CAH water decreases when the CAH water flow increases. But the increase of CAH water flow is not proportional to the increase of CA humidity, it's an upward process with a decreasing slope which also illustrates the change in humidification efficiency.

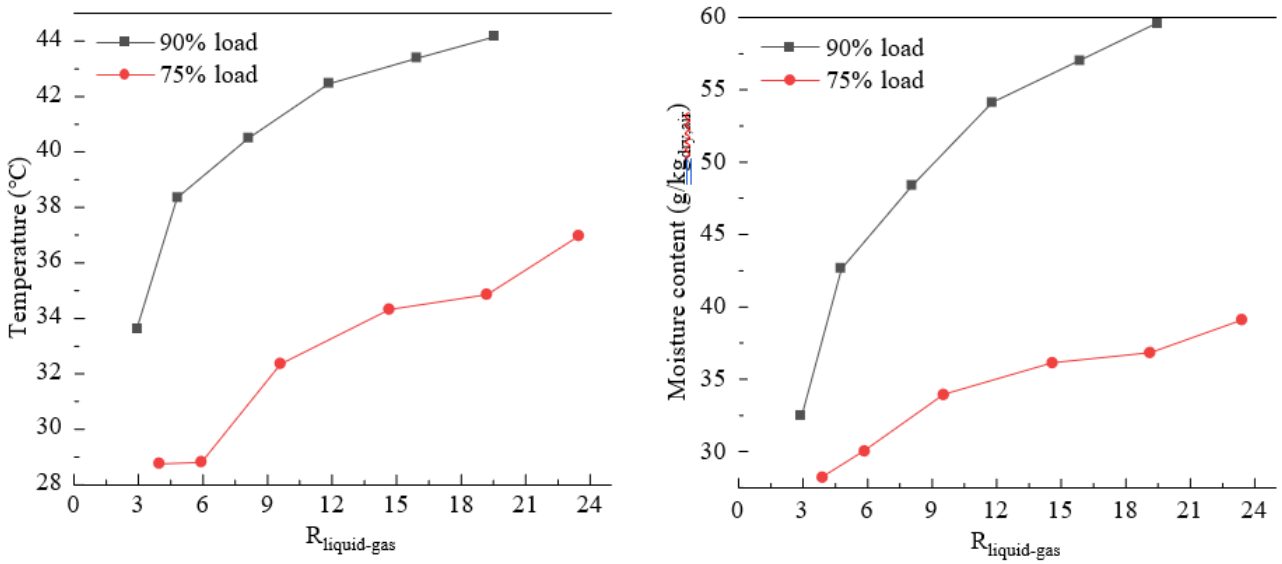

(a) **(b)**

Fig.4 Influence of the $R_{liquid-gas}$ on CA temperature (a) and moisture content (b) after humidification

3.1.2 Heat Transfer in the Humidification Process

The experimental data shows the heat transfer in the CAH tower, as shown in **Figure 5**. Under the experimental conditions, the highest heat gain of CAH water is 4.11kW. The heat gain of CA is the highest under the same condition, which is 3.48kW. Increase of the $R_{liquid-gas}$ has a positive effect on the heat gain of CAH water and the heat gain of CA.

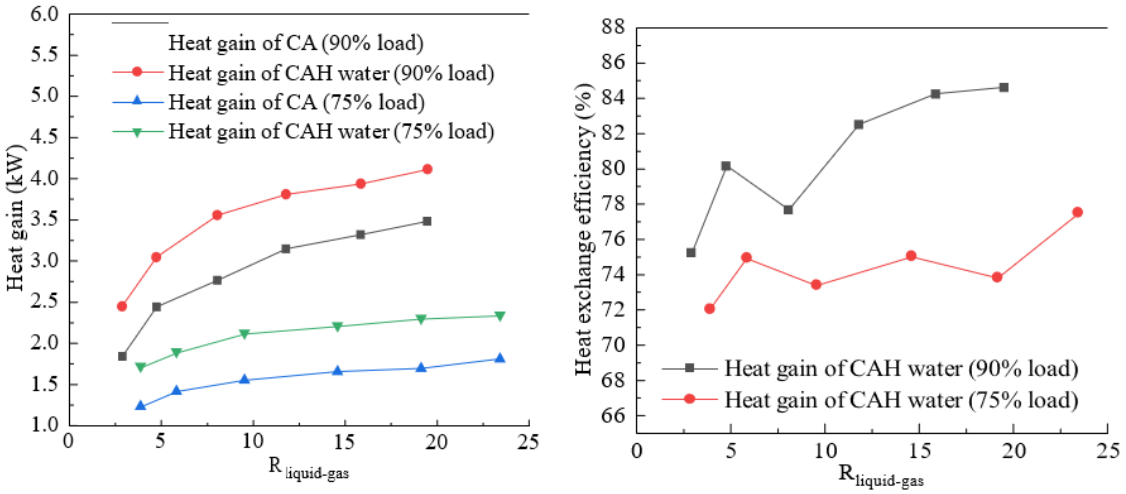

(a) **(b)**

Fig 5. Influence of the $R_{liquid-gas}$ on heat exchange in the CAH tower (a) and exchange efficiency (b)

The heat exchange efficiency in the CAH tower is always higher than 75% under the 90% boiler load condition, and higher than 70% under the 75% boiler load condition. The highest efficiency occurs when the $R_{liquid-gas}$ is max, which is 84.58% under the 90% load and 77.46% under the 75% load. The maximum heat loss in this process occurs when $R_{liquid-gas}$ is 9.57, which is 0.8kW. In most cases, the heat loss in the CAH tower under the 90% load is 0.6-0.7kW, which is 0.5-0.6kW under the 75% load.

3.2 NOx Emissions of gas Boiler

The humidified CA entered the boiler can reduce the concentration of O_2 and natural gas, which can inhibits combustion process in boiler(Kapusuz et al., 2018). The temperature in the combustion chamber is reduced, which effectively suppresses the generation of thermal NOx(Turns, 1995). The NOx content in the flue gas was negatively correlated with the moisture content of the CA.

In experiment, minimal NOx emissions occured under the condition of maximum CAH water flow. The NOx emissions can be reduced by 58.28%, from 100.66 mg/m^3 to 39.66 mg/m^3. The NOx content in the flue gas presents two trends in **Figure 6 (a)**. The reduction rate of NOx is faster when $R_{liquid-gas}$ is from 0 to 3, but it slows down significantly when $R_{liquid-gas}$ is more than 3. The increase of CAH water content had a non-linear effect on NOx emissions. However, it seems to be a certainlinear relationship when observed the change of NOx emissions with the moisture content of the CA. In fact, limited by the CAH water temperature, the moisture content of the CA cannot increase infinitely with the increase of CAH water flow. Thedecline of humidification efficiency also leads to the change of NOx under a higher $R_{liquid-gas}$ is not as obvious as that it under a lower $R_{liquid-gas}$.

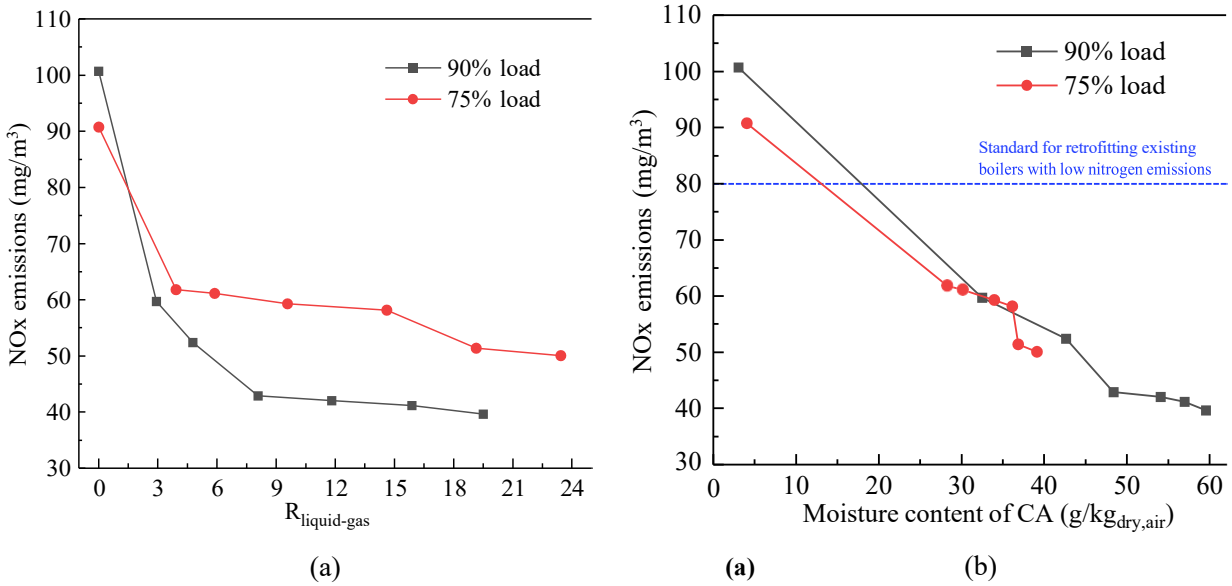

Fig.6 Influence of the $R_{liquid-gas}$ of CAH tower (a) and the moisture content of CA (b) on NOx emissions

The heat and mass exchange process in the CAH tower is more obviously affected by the CAH water temperature. We found

that the CAH water temperature at low load is always lower than that at high load, which leads to better NOx reduction effect when the system is running at high load. When the $R_{liquid-gas}$ is more than 3, it can meet the current emission standards for the retrofit of old gas boilers in China. In fact, the lowest NOx emissions achieved within the experimental range can meet the emission standards for new gas boilers in some Chinese cities, too.

Taking the need for clean emissions into account, this system is actually more suitable for long-term high-load operation. We believe that it's more suitable for use as a main heat source rather than a peak-shaving heat source.

3.3 Heat Transfer Process in WHR Tower

3.3.1 Heat Recovery Process of the HP

The WHR performance of the system was tested under the conditions of the maximum CAH water flow, which means that low NOx emissions were taken into account. Since the heat entered the CAH water circulates continuously in the path: CAH tower - boiler – flue gas - FTHE - CAH tower, this part of the heat is only used to increase the temperature and moisture content of the CA to achieve better NOx reduction effect. To improve the heating efficiency, HP is used to absorb the WH from the flue gas and transfer it to the heat network. Under the 90% load, the performance of the HP was recorded, as shown in **Table 6**.

Table 6. Influence of WHR water temperature and flow on WHR performance of HP

CAH water temperature	WHR water flow	Inlet temperature	Outlet temperature	HP power consumption	Exhaust gas temperature	Heat gain of WHR water	HP COP
℃	L/h	℃	℃	kW	℃	kW	
40	160	39.43	53.71	2.09	32.55	2.67	1.28
	400	40.33	48.16	1.92	28.08	3.66	1.91
	800	39.59	44.57	1.81	25.44	4.65	2.34
	1,200	39.29	42.96	1.77	24.62	5.13	2.51
	1,853	39.55	42.01	1.74	24.46	5.32	2.56
45	160	44.27	58.00	2.22	34.13	2.56	1.16
	400	44.36	51.40	2.02	31.33	3.29	1.62
	800	44.38	48.77	1.95	29.65	4.10	2.10
	1,200	44.15	47.47	1.93	29.11	4.65	2.41
	1,859	44.08	46.38	1.92	28.50	4.99	2.60
50	160	49.10	62.27	2.28	36.34	1.68	1.08
	400	49.56	54.94	2.17	33.16	2.51	1.16
	800	49.76	53.16	2.15	31.85	3.18	1.48
	1,200	49.79	52.24	2.09	31.93	3.44	1.64
	1,781	49.91	51.64	2.08	31.33	3.59	1.73

When the WHR water flow is low, the effect of WHR water temperature on WHR efficiency is relatively limited. Most of the heat gained by the heat network comes from the power consumption of the compressor, and the COP is close to 1. The HP cannot absorb any heat in the flue gas. Therefore, the operating conditions of low WHR water flow should be avoided. Under

high WHR water flow conditions, colder WHR water can get more heat from flue gas. The maximum value of heat gain from flue gas occurs under the WHR water condition of 40°C and 1,853 L/h, which is 3.58kW. The WHR efficiency can reach 6.94% at the highest.

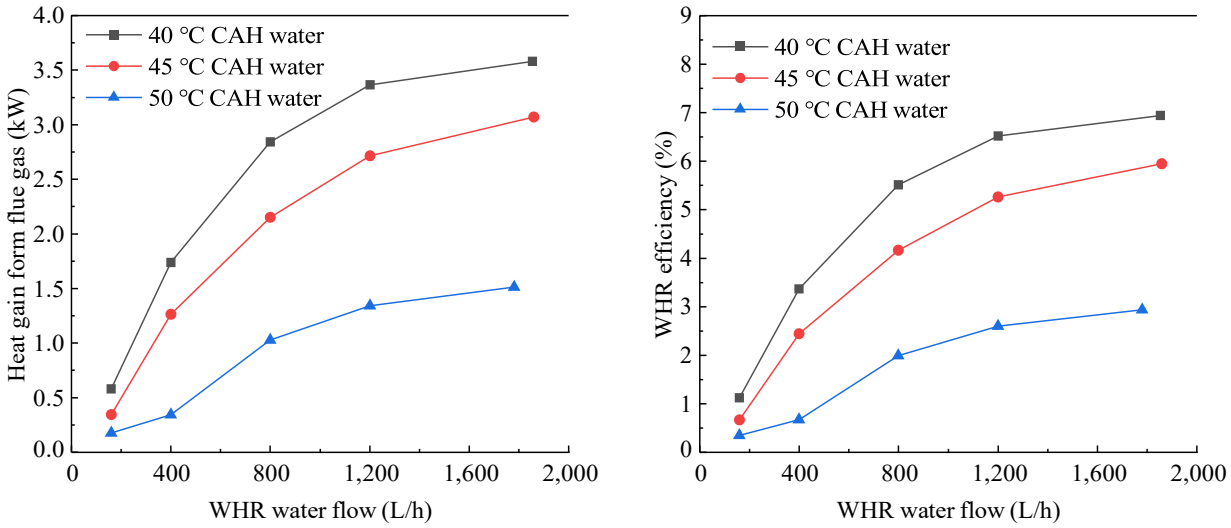

(a) (b)

Fig.7 The effect of WHR water temperature and flow on WHR (a) and its efficiency (b)

The heat gain of WHR water is affected by its flow rate and temperature. Although the increase in WHR efficiency becomes less pronounced as the WHR water flow increasing, a lower water temperature can obviously solve this problem.

3.3.2 Influence of Humidification Conditions on WHR Process

Humidified CA increases the vapor content in the furnace. These vapor will flow out with the flue gas, so that the dew point temperature of the flue gas is increased, as shown in **Figure 8 (a)**. The higher dew point temperature effectively reduces the difficulty of recovering latent heat, which has an enhanced effect on the heat exchange process inside the WHR tower.

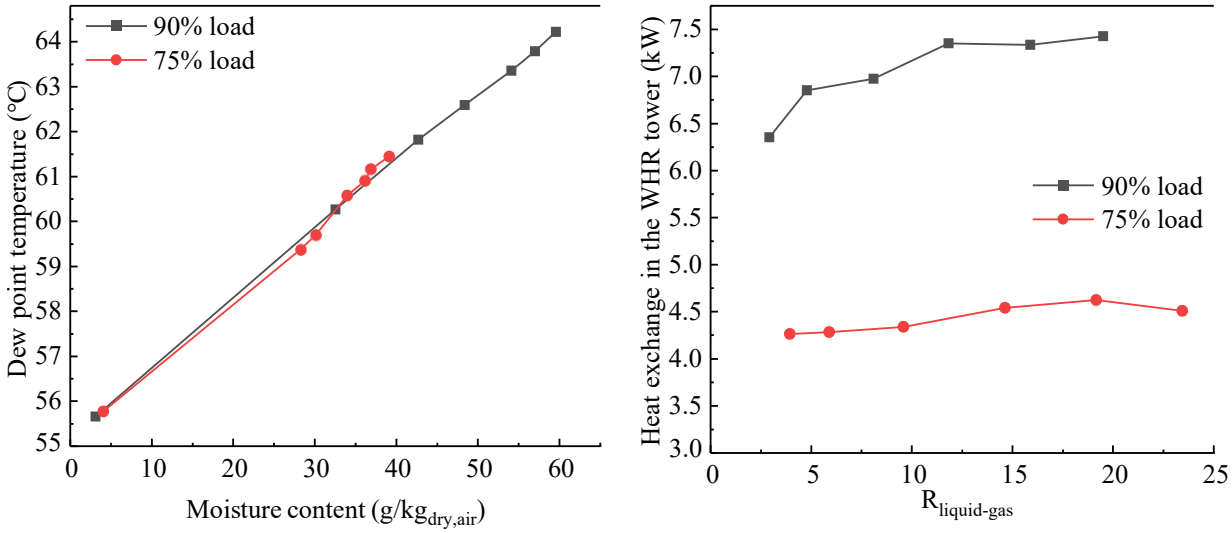

(a) **(b)**

Fig.8 Flue gas dew point under the different moisture content of CA (a) and total heat enchange in WHR tower under the different $R_{liquid-gas}$

In the WHR tower, the heat of the flue gas is absorbed by the CAH water and HP. Due to the increase in dew point temperature,

the heat exchanged in the WHR tower increases, as shown in **Figure 8 (b)**. These data were measured under the HP optimal operating conditions. The results show that the increase of the $R_{liquid-gas}$ has an enhanced effect on the heat transfer in the WHR tower, which is 1.08kW increased under 90% load and 0.36KW increased under 75% load. As the temperature of the flue gas is always reduced below the dew point in the WHR tower, the WHR process always takes place sufficiently, which results in an insignificant variation of the heat exchange in the WHR tower with the change of $R_{liquid-gas}$.

Both CAH water and WHR water participate in the heat exchange process of the WHR tower, which inevitably lead to competition for heat between them. As shown in **Figure 9 (a)**, the effect of this competition on the HP has been shown to be stronger than the rise in the dew point of the flue gas, which leads to a negative impact of humidification on HP performance. This effect is more pronounced when the boiler load is high: WHR efficiency was reduced by 1.34% under 90% load and 0.37% under 75% load.

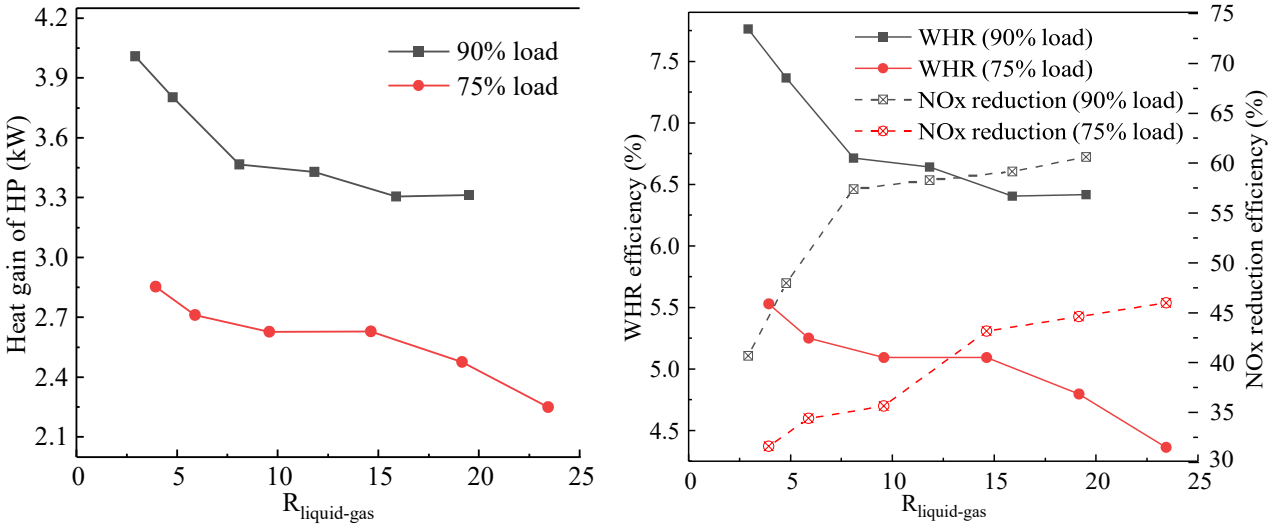

(a) (b)

Fig.9 Heat gain of HP (a), the relationship between NOx reduction and WHR (b) under the different $R_{liquid-gas}$

The NOx reduction efficiency here is calculated as a ratio of the reduction in emissions to the NOx emissions without humidification under the same load. Therefore, there is a conflict between NOx reduction and WHR, as shown in **Figure 9 (b)**. The NOx reduction efficiency increases as the CAH water flow rate increases, but the CAH water absorbs too much heat, resulting in less heat can be recovered by the HP.

4. System Assessment

4.1 Energy-saving Analysis

High CAH water flow, high WHR water flow and low WHR water temperature were previously shown to be beneficial for flue gas heat transfer. The exhaust gas temperature under 90% load and the maximum CAH water flow was tested, as shown in **Figure 10**. The exhaust gas temperature of the system can reach the lowest value of 24.46℃.

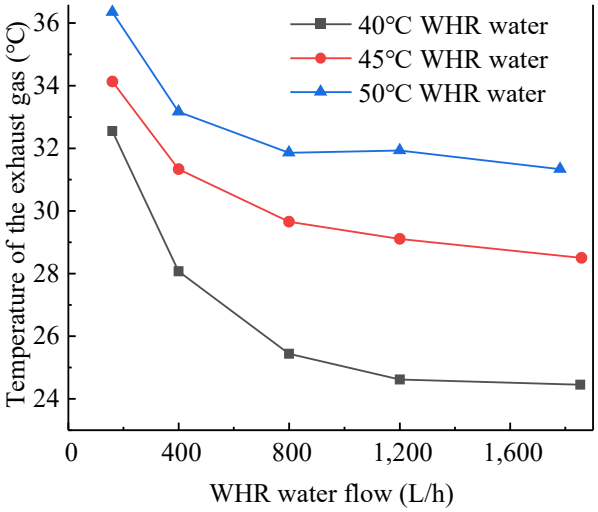

Fig.10 The influence of WHR water flow on boiler exhaust gas temperature

In addition, the humidified CA has an effect on the heating efficiency of the boiler. As shown in **Figure 11 (a)**, 40℃ back water in heat network was used to absorb heat, the change of heating efficiency shows a decreasing trend as the $R_{liquid-gas}$ gradually increased to its maximum value. This finding is consistent with the study by Ji (Ji et al., 2019). The heating efficiency decreased by 3.39% and 4.36% under different loads. That is the price of NOx reduction.

In the experiments, the heating efficiency of the system was always higher than that of original boiler. The orange area in **Figure 11(b)** shows the reason: the additional heat from flue gas was sent to the heat network by HP.

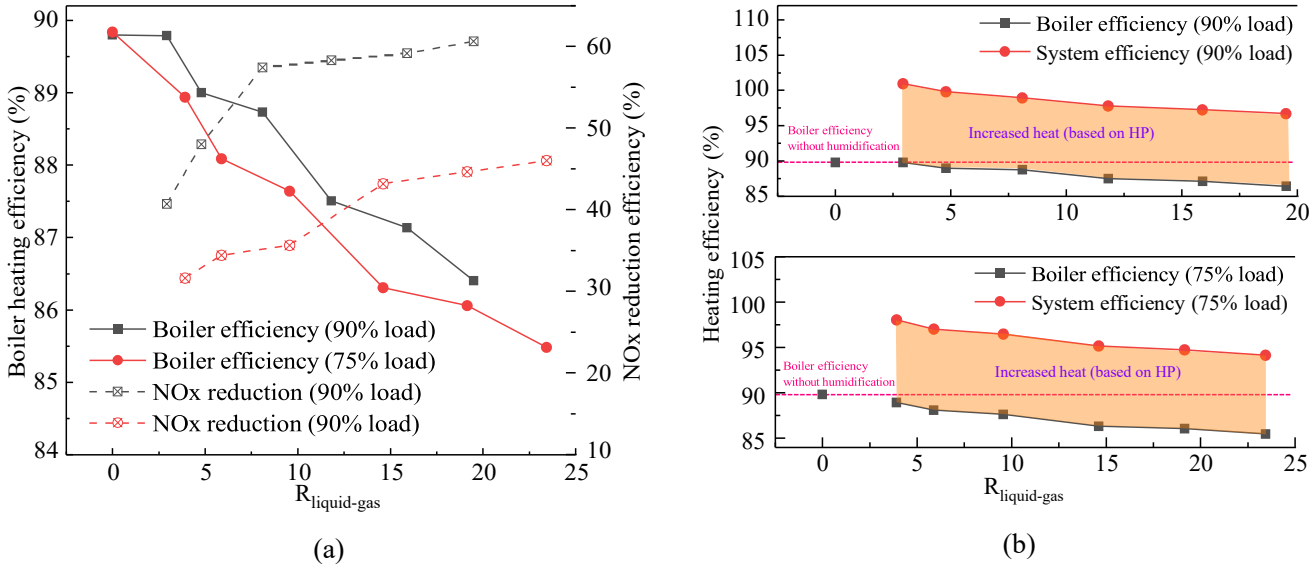

Fig.11 Heating efficiency of the boiler and the system under the different $R_{liquid-gas}$

The energy entered by the system comes from gas, CA, water pumps, fans, and HP. The WH of the flue gas is used to improve the heat and mass exchange efficiency in the CAH tower and heating back water of the heat network. The diagram of energy flow under the condition of 90% load, 1,537 L/h CAH water flow, 1,858 L/h WHR water flow, and 40 °C WHR water temperature is shown in **Figure 12 (a)**.

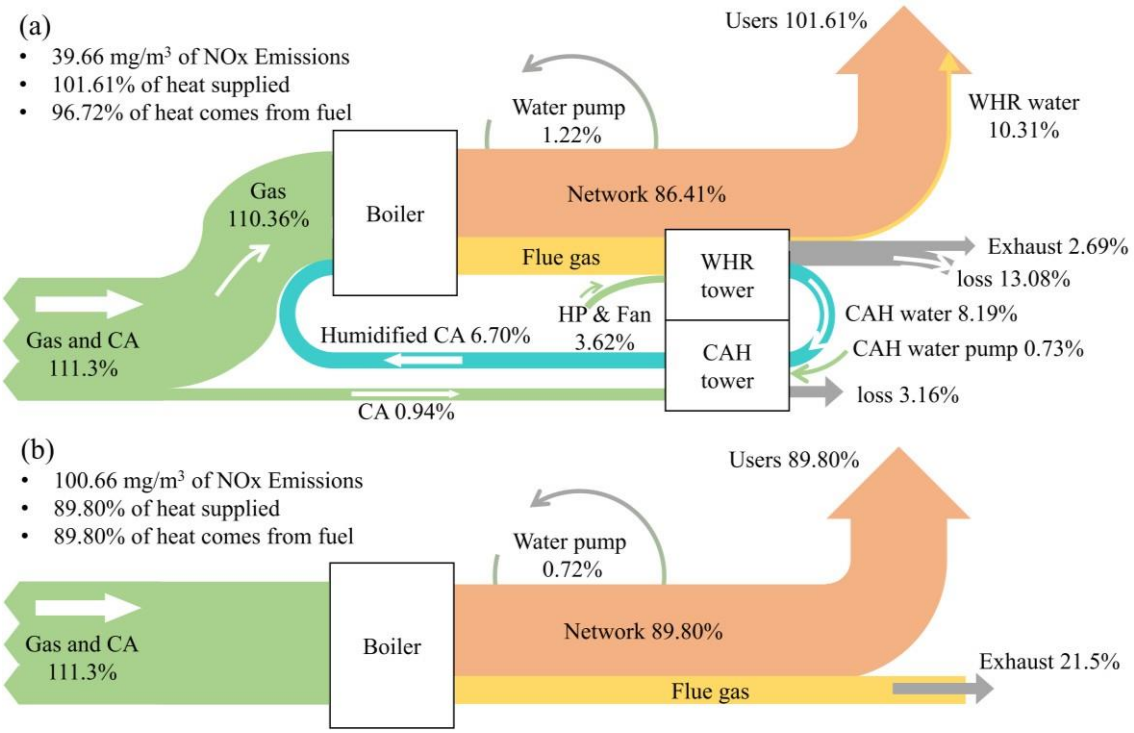

Fig.12 Energy-flow diagram: boiler with (a) or without (b) two towers

In the WHR tower, the CAH water absorbs 8.19% of the energy and transfers it in the CAH tower. This process requires 0.73% of the energy provided by pump. 10.31%of the energy is transmitted to the heat net by the HP. Flue gas is discharged by fan. The utilization of WH has two effects: reinforcing the moisture content of the CA and then reducing NOx emissions; increasing the heat of the heat network. Due to the improvement of the flow resistance of heat network water, the energy consumption of additional heat network water pump has been increased.

The CAH water pump is used to drive the flow of CAH water, and these water will enter the CAH tower with 8.19% of the energy. CA can get 5.76% of the energy in the CAH Tower. The energy loss of the whole CAH tower is 3.16%. Excessive vapour entered the boiler causes two consequences: lower NOx production and lower boiler efficiency from 89.90% to 86.41%. In addition, due to the maximum WHR water flow, the energy consumption of the heat network water pump is further increased, which is only used to maintain the flow of heat network water.

The heat in the exhaust gas only accounts for 2.69%, but the heat loss in the WHR tower reaches 13.08%, which includes the heat taken away by the condensed water. The heat loss of the whole system is mainly concentrated in the WHR tower. The use of materials with better thermal insulation performance will effectively reduce this part of the loss.

4.2 Environmental Analysis

The HP increases the total heat input of the boiler system into the heat network. The increase in overall heating efficiency means less gas consumption and NOx generation. Lower fuel consumption also effectively reduces the CO_2 generation of the system if the electricity used to drive the HP comes from a regional renewable energy grid.

The NOx and water-savings of the system are shown in **Figure 13**. High $R_{liquid-gas}$ has a positive effect on NOx reduction

and the amount of condensed water. If the boiler system only operates for one heating season per year (121 days), the NOx emission reduction of the boiler system is 65.18-117.87 kg/a, which varies according to the change of operating conditions. Due to the comprehensive heat exchange in the WHR tower, most of the vapor in the flue gas can be condensed, which is 20.15-31.22 t/a.

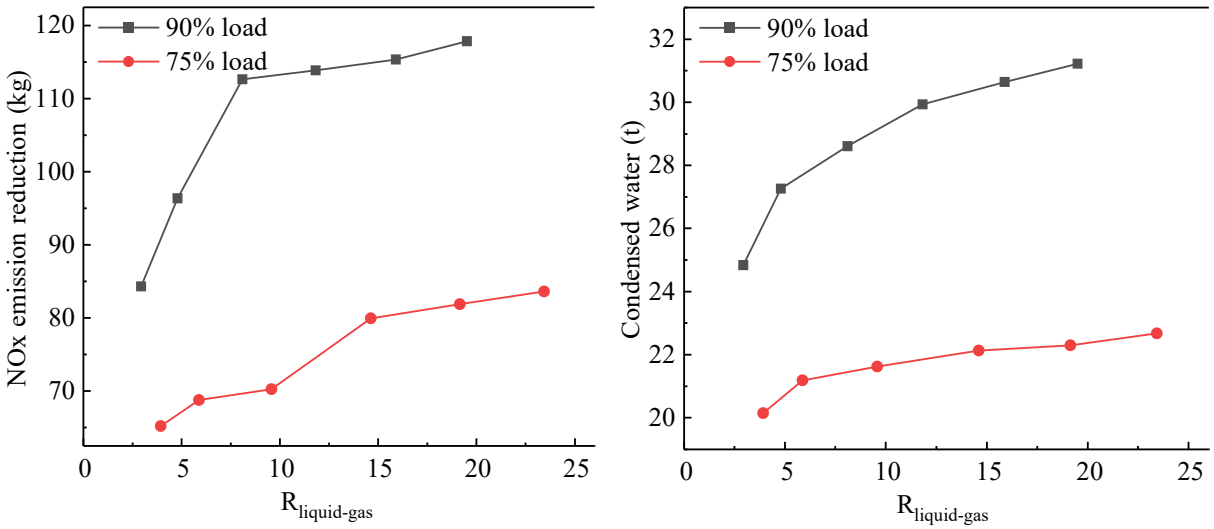

(a) (b)

Fig.13 The Annual NOx emission reduction (a) and water-savings (b)

4.3 Economic Analysis

Under the condition of a specific heat demand, the system can reduce the running time through HP, as shown in **Table 7**.

Table 7. The comparison of running time with and without HP (h/day)

Running time（system）		WHR water temperature (℃)		
		40	45	50
WHR water flow (L/h)	160	9.18	10.22	11.56
	400	8.86	10.01	11.50
	800	8.59	9.75	11.29
	1200	8.46	9.60	11.21
	180	8.47	9.46	11.19
Running time（just boiler）		WHR water temperature (℃)		
		40	45	50
WHR water flow (L/h)	160	9.73	10.88	12.37
	400	9.57	10.83	12.33
	800	9.47	10.75	12.32
	1200	9.41	10.71	12.31
	180	9.46	10.62	12.34

The main energy benefit of the system is calculated by the gas-savings. The unit price of gas refers to the relevant standards of Beijing, which is 2.88CNY/Nm^3. On the premise of maintaining low NOx emissions, the gas-savings of the system under different WHR water flow rates and temperatures were tested, as shown in **Figure 14**. WHR water is taken from the back water of the heat network. An increase in its temperature results in a decrease in heat transfer within the boiler. Compared

with WHR efficiency, boiler efficiency decreases more obvious when the back water temperature is higher, which means the recovered WH accounts for a larger proportion of the total heat gain of the heat network. The recovered WH is intuitively reflected in the reduction of system running time. Since the input flow of gas is constant, this effect is reflected in the cost.

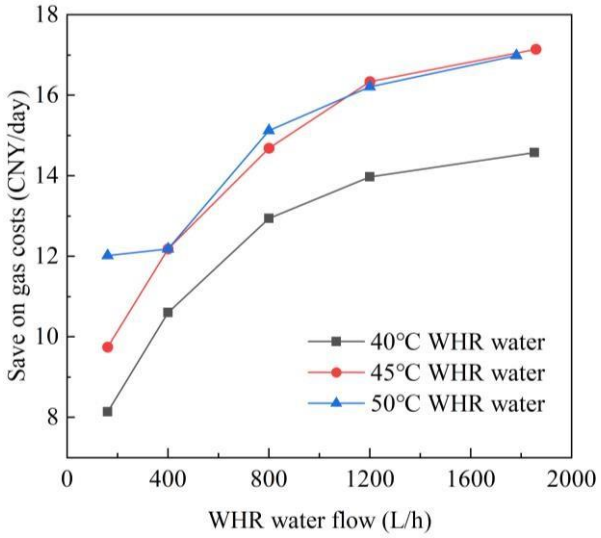

Fig.14. Economic benefits based on increased heating efficiency

The additional energy consumption of the system is mainly electrical energy. The unit price of electricity in Beijing is adjusted according to the time of using electricity, which are 1.0337, 0.9440, 0.6346 and 0.3342 CNY/kW*h respectively. Each of them lasts 6 hours. The running time of the system is 8-12 hours. Therefore, the minimum power consumption cost is used as the operating strategy.

The energy consumption of the CAH water pump and fan is 0.37 kW and 0.13 kW. The main reason for the increase in power consumption of the heat network water pump is that the WHR water flows through the HP evaporator. As the WHR water flow through the condenser continues to increase, the power of the water pump is gradually increased. Additional costs caused by system operation are shown in **Figure 15**.

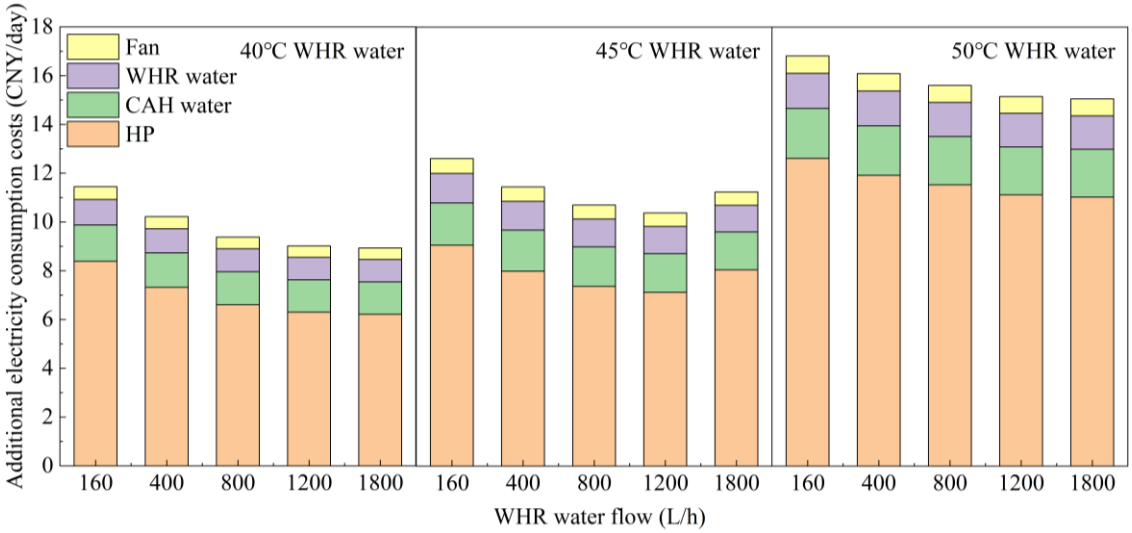

Fig.15. Additional energy consumption of the system

The reduction of WHR water temperature and the increase of WHR water flow can significantly reduce system operating costs. To calculate the payback period, the costs of equipments that make up the system are shown in **Table 8**.

Table 8. Initial investment in equipment

Equipment	quantity	Total price (CNY)
CAH tower	1	1,100
HP (without evaporator)	1	2,430
Direct expansion evaporator	1	900
Finned tube heat exchanger	1	500
Water pipes and fittings	Several	500
Water pump	1	775
Distribution control system	1	836
other		500
total		7540

The payback period of the system is shown in **Table 9**. In the conditions of higher WHR water flow and lower temperature, the payback period of the system is short. It is worth noting that the shortest payback period occurs at 45°C WHR water condition. But this calculation only considers the relative gas-saving under the same working condition, and does not consider the actual gas consumption under different working conditions. Considering the system efficiency and gas consumption, the condition of 40°C and 1800L/h WHR water is recommended. The payback period of the system is not short, considering various types of labor costs, this system is more suitable for use in regions with encouragement of clean production policies.

Table 9. Payback period of the system (a)

WHR water temperature (°C)	WHR water flow (L/h)				
	160	400	800	1200	1800
40	-	163.29	17.50	12.57	11.04
45	-	84.25	15.65	10.46	10.56
50	-	-	-	59.19	32.23

5. Conclusions

The synergy system integrating HP and humidification combustion meets the needs of gas boilers for efficient operation and exhaust purification. In the experiments, the system performance, synergistic working mechanism and applicability are elaborated. Conclusions are as follows:

1) Increasing the flow of CAH water can increase the humidity of the CA, thereby reducing the production of NOx. The moisture content of CA is largely dependent on the temperature of the CAH water, and the flow rate is often excessive. The maximum moisture content of the CA is 59.54 $g/kg_{dry,air}$, and the NOx content of the exhaust gas is 39.66 mg/m^3, which is 62.35% NOx reduction efficiency.
2) Humidification combustion reduces the heating efficiency of the boiler. The highest efficiency reduction under experimental conditions was 3.49%. The HP increases the amount of heat gain of heat network. Even at the lowest NOx emission conditions, the heat gain of the heating network is also higher than that without humidification.
3) The increase of the $R_{liquid-gas}$ increases the dew point temperature of the flue gas, which is beneficial to enhance the heat exchange in the WHR tower. It is reflected in a slight reduction in heat gain for HP, but a significant increase in heat gain for CAH water. When the system is turned on, the exhaust gas temperature is always maintained below 40 °C, and

the lowest temperature is 24.46 °C.

4) The heat recovered by HP is maximized under the condition of highest WHR water flow and the lowest WHR water temperature. The heat absorption by the HP are also affected by $R_{liquid-gas}$. Under the optimal condition, 6.42% of the heat from the flue gas is recovered by HP, which effectively compensates for the decrease in heating efficiency caused by NOx reduction.
5) The maximum NOx emissions reduction is 117.87 kg in one heating season, and 31.22 tons of condensed water can be recovered. Considering the payback time, this system is more recommended to use it in areas with policy support.

Considering that the NOx emission of the system is affected by the boiler load, the boiler system should be used as a primary heat source instead of a peak-shaving heat source in order to ensure lower NOx emissions. There is obvious heat loss in the WHR tower. The utilization of this heat can effectively improve the thermal efficiency and NOx reduction rate. The payback time will also be shortened.

6. future works

The experimental system has relatively serious heat loss. The NOx emissions and thermal efficiency of the system will be tested after the thermal insulation measures of WHR tower are optimized.

The completed works are rarely involved in the research of emissions and energy efficiency under variable working conditions. Although we believe that the reduction of the mass transfer rate in the CAH tower at low load will affect the NOx reduction efficiency of the system, it still has the potential to be regulated with reference to users' load when applied to existing gas boilers. The variable operating condition analysis of the system will be tested.

3E analysis cannot directly compare the environmental benefits of NOx reduction with the economic benefits of efficiency improvements. This has great limitations on the regulation of the system: we can only determine the operating conditions with the highest NOx reduction efficiency or the highest thermal efficiency. It is difficult to know whether heating efficiency or nitrogen reduction levels are more important for health effects. Future work will start from Emergy analysis.

References

November 14, 2022. Calculation of wet air physical properties. http://www.ap1700.com/MoistAir.htm.

ASHRAE, 2013. 2013 ASHRAE HANDBOOK FUNDAMENTALS. American Society of Heating Refrigerating and Airconditioning Engineer.

Cai, Y., Sam, C.Y., Chang, T., 2018. Nexus between clean energy consumption, economic growth and CO2 emissions. Journal of Cleaner Production 182, 1001-1011.

Cansino, J.M., Moreno, R., Quintana, D., Roman-Collado, R., 2019. Health and Heating in the City of Temuco (Chile). Monetary Savings of Replacing Biomass with PV System in the Residential Sector. SUSTAINABILITY 11(19).

Carroll, J.P., Finnan, J.M., Biedermann, F., Brunner, T., Obernberger, I., 2015. Air staging to reduce emissions from energy crop combustion in small scale applications. Fuel 155, 37-43.

Chen, H., He, L., Chen, J., Yuan, B., Huang, T., Cui, Q., 2019. Impacts of Clean Energy Substitution for Polluting Fossil-Fuels in Terminal Energy Consumption on the Economy and Environment in China. Sustainability 11(22), 6419.

Chen, H., Zhou, Y., Cao, S., Li, X., Su, X., An, L., Gao, D., 2017. Heat exchange and water recovery experiments of flue gas with

using nanoporous ceramic membranes. Applied Thermal Engineering 110, 686-694.
Chen, W., Shi, W., Wang, B., Shang, S., Li, X., 2017. A Deep Heat Recovery Device between Flue Gas and Supply Air of Gas-fired Boiler by Using Non-contact Total Heat Exchanger. Energy Procedia 105, 4976-4982.
Cheng, G., Zhang, C., 2018. Desulfurization and Denitrification Technologies of Coal-fired Flue Gas. Polish Journal of Environmental Studies 27(2), 481-489.
El Sheikh, K., Khan, M.J.H., Diana Hamid, M., Shrestha, S., Ali, B.S., Ryabov, G.A., Dolgushin, L.A., Hussain, M.A., Bukharkina, T.V., Gorelova, E.A., 2019. Advances in reduction of NO and N2O1 emission formation in an oxy-fired fluidized bed boiler. Chinese Journal of Chemical Engineering 27(2), 426-443.
Feser, J.S., Gupta, A.K., 2018. Effect of CO2/N-2 Dilution on Premixed Methane-Air Flame Stability Under Strained Conditions. Journal of Energy Resources Technology-Transactions of the Asme 140(7).
Gamrat, S., Poraj, J., Bodys, J., Smolka, J., Adamczyk, W., 2016. Influence of external flue gas recirculation on gas combustion in a coke oven heating system. Fuel Processing Technology 152, 430-437.
Glen, S., April 14, 2021. Error Propagation (Propagation of Uncertainty). https://www.statisticshowto.com/statistics-basics/error-propagation/.
Hebenstreit, B., Schnetzinger, R., Ohnmacht, R., Höftberger, E., Lundgren, J., Haslinger, W., Toffolo, A., 2014. Techno-economic study of a heat pump enhanced flue gas heat recovery for biomass boilers. Biomass and Bioenergy 71, 12-22.
Hu, B., Liu, H., Jiang, J., Zhang, Z., Li, H., Wang, R.Z., 2022. Ten megawatt scale vapor compression heat pump for low temperature waste heat recovery: Onsite application research. Energy 238.
IHME, 2019. GBD Compare, in: Washington, U.o. (Ed.). University of Washington.
Ji, W., Li, A., Lu, X., Huang, Z., Zhu, L., 2019. Numerical study on NOx and ISFC co-optimization for a low-speed two-stroke engine via Miller cycle, EGR, intake air humidification, and injection strategy implementation. Applied Thermal Engineering 153, 398-408.
Kapusuz, M., Cakmak, A., Ozcan, H., 2018. Emissions analysis of an SI engine with humidified air induction, International Scientific Conference on Environmental and Climate Technologies (CONECT). Riga, LATVIA, pp. 235-241.
Khaled, M., Ramadan, M., 2017. Study of the Thermal Behavior of Multi Tube Tank in Heat Recovery from Chimney—Analysis and Optimization. Heat Transfer Engineering 39(5), 399-409.
Kuck, J., 1996. Efficiency of vapour-pump-equipped condensing boilers. Applied Thermal Engineering 16(3), 233-244.
Lee, C.-E., Kim, D.-H., 2020. Heat recovery boilers with water spray. Part I: Thermodynamic analysis validation and boiler practicality. Thermal Science and Engineering Progress 18.
Li, Z., Hu, R., Xie, P., Chen, H., Liu, X., Liang, S., Wang, D., Wang, F., Wang, Y., Lin, C., Liu, J., Liu, W., 2019. Simultaneous measurement of NO and NO₂ by a dual-channel cavity ring-down spectroscopy technique. Atmospheric Measurement Techniques 12(6), 3223-3236.
Lion, S., Vlaskos, I., Taccani, R., 2020. A review of emissions reduction technologies for low and medium speed marine Diesel engines and their potential for waste heat recovery. Energy Conversion and Management 207.
Lu, D., Chen, G., Gong, M., Bai, Y., Xu, Q., Zhao, Y., Dong, X., Shen, J., 2019. Thermodynamic and economic analysis of a gas-fired absorption heat pump for district heating with cascade recovery of flue gas waste heat. Energy Conversion and Management 185, 87-100.
Men, Y., Liu, X., Zhang, T., 2021. A review of boiler waste heat recovery technologies in the medium-low temperature range. Energy 237.
Qu, M., Abdelaziz, O., Yin, H., 2014. New configurations of a heat recovery absorption heat pump integrated with a natural gas boiler for boiler efficiency improvement. Energy Conversion and Management 87, 175-184.
Roman-Collado, R., de Reyna, J.J., 2019. The economic benefits of fulfilling the World Health Organization's limits for particulates: A case study in Algeciras Bay (Spain). JOURNAL OF THE AIR & WASTE MANAGEMENT ASSOCIATION 69(4), 438-449.
Shahpouri, S., Houshfar, E., 2019. Nitrogen oxides reduction and performance enhancement of combustor with direct water injection and humidification of inlet air. Clean Technologies and Environmental Policy 21(3), 667-683.
Shang, S., Li, X., Chen, W., Wang, B., Shi, W., 2017. A total heat recovery system between the flue gas and oxidizing air of a gas-fired boiler using a non-contact total heat exchanger. Applied Energy 207, 613-623.
Shi, B., Hu, J., Peng, H., Ishizuka, S., 2018. Effects of internal flue gas recirculation rate on the NO emission in a methane/air

premixed flame. Combustion and Flame 188, 199-211.
Sidorkin, V.T., Bersenev, K.G., Tugov, A.N., Vereshchetin, V.A., 2019. Formation of Nitrogen Oxides in Combustion of Pyrolysis Gases in Air Heavily Diluted with Recirculating Flue Gas. Thermal Engineering 66(1), 55-62.
Su, Z., Zhang, M., Xu, P., Zhao, Z., Wang, Z., Huang, H., Ouyang, T., 2021. Opportunities and strategies for multigrade waste heat utilization in various industries: A recent review. Energy Conversion and Management 229.
Terhan, M., Comakli, K., 2016. Design and economic analysis of a flue gas condenser to recover latent heat from exhaust flue gas. Applied Thermal Engineering 100, 1007-1015.
Turns, S.R., 1995. Understanding NOx formation in nonpremixed flames: Experiments and modeling. Progress in Energy and Combustion Science 21(5), 361-385.
van de Bor, D.M., Infante Ferreira, C.A., Kiss, A.A., 2015. Low grade waste heat recovery using heat pumps and power cycles. Energy 89, 864-873.
Vandel, A., Chica Cano, J.P., de Persis, S., Cabot, G., 2020. Study of the influence of water vapour and carbon dioxide dilution on flame structure of swirled methane/oxygen-enriched air flames. Experimental Thermal and Fluid Science 113.
Wang, Q., Chen, Z., Han, H., Zeng, L., Li, Z., 2019. Experimental characterization of anthracite combustion and NO emission for a 300-MWe down-fired boiler with a novel combustion system: Influence of primary and vent air distributions. Applied Energy 238, 1551-1562.
Wang, Y., Zhao, Q., Zhou, Q., Kang, Z., Tao, W., 2013. Experimental and numerical studies on actual flue gas condensation heat transfer in a left–right symmetric internally finned tube. International Journal of Heat and Mass Transfer 64, 10-20.
Wei, M., Zhao, X., Fu, L., Zhang, S., 2017. Performance study and application of new coal-fired boiler flue gas heat recovery system. Applied Energy 188, 121-129.
Wu, J., Zhao, K., Li, X., Wang, M., Ni, S., 2020. Numerical study on staged combustion technology in burner of gas-fired boiler. Energy Sources, Part A: Recovery, Utilization, and Environmental Effects, 1-14.
Yang, B., Jiang, Y., Fu, L., Zhang, S., 2018. Conjugate heat and mass transfer study of a new open-cycle absorption heat pump applied to total heat recovery of flue gas. Applied Thermal Engineering 138, 888-899.
Yi, Z., Zhou, Z., Tao, Q., Jiang, Z., 2019. Experimental and Numerical Investigations in a Gas-Fired Boiler With Combustion Stabilizing Device. Journal of Energy Resources Technology 141(11).
Zhang, Q., Niu, Y., Yang, X., Sun, D., Xiao, X., Shen, Q., Wang, G., 2020. Experimental study of flue gas condensing heat recovery synergized with low NOx emission system. Applied Energy 269.
Zhao, X., Fu, L., Yuan, W., Li, F., Li, Q., 2016. The Potential and Approach of Flue Gas Waste Heat Utilization of Natural Gas for Space Heating. Procedia Engineering 146, 494-503.
Zhou, T., Geng, P., Lu, X., 2021. Numerical Simulation of Marine Diesel Engine Combustion and Emissions Using Intake Air Humidification at the Different Injection Timing. Combustion Science and Technology, 1-21.
Zhu, K., Xia, J., Xie, X., Jiang, Y., 2014. Total heat recovery of gas boiler by absorption heat pump and direct-contact heat exchanger. Applied Thermal Engineering 71(1), 213-218.

Declaration of interests

☒ The authors declare that they have no known competing financial interests or personal relationships that could have appeared to influence the work reported in this paper.

☐ The authors declare the following financial interests/personal relationships which may be considered as potential competing interests: